ACS NANO

www.acsnano.org

PERSPECTIVE

Direct Electroreduction of Low-Concentration CO_2: Progress and Perspective

Jing-Jing Li,[▽] Xue-Rong Qin,[▽] Xiao-Ran Wang, Lin-Lin Wang, Zi-You Yu,* and Tong-Bu Lu*

Cite This: *ACS Nano* 2025, 19, 10620−10629

Read Online

ACCESS | Metrics & More | Article Recommendations

ABSTRACT: **The conversion of CO_2 into carbon-based fuels and chemicals via the electrocatalytic CO_2 reduction reaction (CO_2RR) offers an attractive route to reducing the CO_2 emission for carbon neutrality. Currently, high-purity CO_2 gas has been widely used as the feedstock for most of the CO_2RR studies, while CO_2 sources with a typically low concentration impose the extra cost for CO_2 capture and purification steps. The direct utilization of low-concentration CO_2 for the CO_2RR is a promising approach to substantially address this problem. In this Perspective, we first highlight the prominent advantages of direct electroreduction of low-concentration CO_2. Then we focus on the summary of several important design strategies for CO_2RR in diluted CO_2 and gas impurities-containing CO_2 atmosphere. Finally, we propose personal outlooks on future challenges and some opportunities for this fascinating research field.**

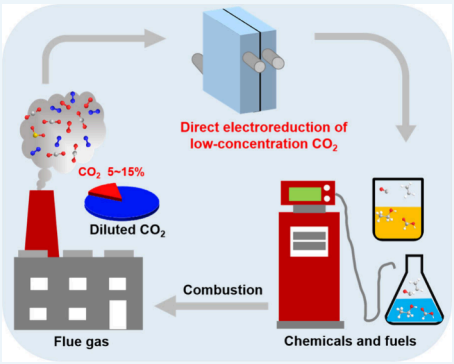

KEYWORDS: *electrocatalytic CO_2 reduction reaction, electroreduction, low-concentration CO_2, gas impurities, design strategies*

1. INTRODUCTION

With the continuous expansion of industrial activities and the increasing combustion of fossil fuels, the concentration of carbon dioxide (CO_2) in the atmosphere is projected to rise to approximately 590 ppm by the end of the century.[1−5] The escalating levels of CO_2 emissions resulting from human activities have caused the increasing challenges of global warming and climate variation owing to the greenhouse effect.[6−11] One efficient approach to lower CO_2 emissions is the utilization of CO_2 for the production of valuable carbon-based fuels. Currently, diverse CO_2 conversion technologies, including electrocatalytic reduction,[12,13] photocatalytic reduction,[14,15] and thermocatalytic reduction,[16,17] have been employed to improve the conversion efficiency. Among them, the use of the electrocatalytic CO_2 reduction reaction (CO_2RR) powered by renewable energy to convert waste CO_2 into value-added chemicals and fuels, such as C_1 products (carbon monoxide, formic acid, methane, and methanol) and C_{2+} products (ethylene, ethanol, acetate, and propanol), has been considered as a very promising pathway and attracted much attention for extensive investigation.[18−24]

Over the past few years, we have witnessed much progress in the study of electrocatalytic CO_2RR, and many designed reactors and catalysts have exhibited excellent CO_2RR performance, including high selectivity, large current density, and good stability.[25−30] To date, the majority of efforts in this field have been conducted to use high-purity CO_2 (>99%) as the reactant streams. However, the primary CO_2 sources such as industrial flue gas from fossil fuel combustion typically contain a low concentration of CO_2 at 5−15%.[31−34] The diluted CO_2 is thus required to experience the capture, enrichment, and purification process to achieve high-purity CO_2 for subsequent use in CO_2RR electrolysis. The process usually takes high energy consumption and extra investment costs, significantly diminishing the economic feasibility for the electrocatalytic CO_2RR technology.[35−37] The direct utilization and electroreduction of low-concentration CO_2 into valuable products holds great potential to bypass these CO_2 purification steps and thus reduce the expended cost. Some attempts and explorations for catalyst design have been made to improve the CO_2RR performance in diluted CO_2 conditions, thus stimulating a review to summarize recent progress and propose future challenges in this field.

In this Perspective, we begin with a brief discussion of the pros and cons of the CO_2RR in pure and diluted CO_2. After that, we systematically summarize several kinds of catalyst design strategies and discuss their structure−performance

Received: January 20, 2025
Revised: March 5, 2025
Accepted: March 6, 2025
Published: March 13, 2025

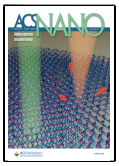

https://doi.org/10.1021/acsnano.5c01268
ACS Nano 2025, 19, 10620−10629

relationship for CO_2RR in diluted CO_2 and gas impurities-containing CO_2 atmospheres. Finally, some main challenges and future possible directions for this research field are put forward.

2. THE PROMINENT ADVANTAGES OF DIRECT ELECTROREDUCTION OF LOW-CONCENTRATION CO_2

Many previous reports rely highly on the use of high-purity CO_2 as the feedstock for the electrocatalytic CO_2RR. It is thus required to enrich and purify the diluted CO_2 to generate pure CO_2, as the CO_2 concentration in industrial flue gas is very low.[4,38−42] Commonly, on the basis of the neutralization reaction between acidic CO_2 gas and the basic solutions, CO_2 gas is first captured by alkaline solutions or amine-based solutions, followed by the subsequent drying and thermal treatments to release the pure CO_2 gas and simultaneously regenerate these adsorbents (Figure 1a).[3,43−45] For example, in

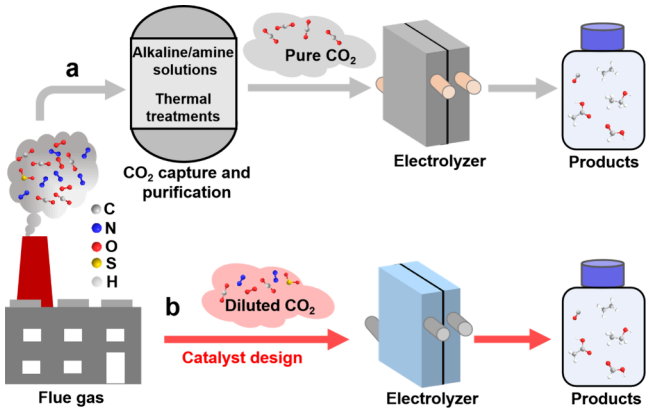

Figure 1. Comparison of the CO_2RR using high-purity and low-concentration CO_2. (a) Schematic illustration of the capture and purification of diluted CO_2 to obtain high-purity CO_2 for electrolysis. (b) Schematic illustration of the direct utilization of diluted CO_2 for electrolysis.

a pilot scale, a popular method is the use of a strongly alkaline NaOH or KOH solution to capture CO_2, owing to the strong CO_2 absorption capability. The obtained alkali carbonate salts will react with $Ca(OH)_2$ to form $CaCO_3$ precipitates, which are subjected to a high-temperature calcination process (>900 °C) to produce the concentrated CO_2 gas.[3,45,46] This calcination process is extremely energy-intensive, making the major proportion of the total energy consumption.[39,47] Techno-economic analysis reveals that the cost for CO_2 purification through the current method can reach as high as $70−100 per ton of CO_2, which even accounts for 30−50% of the overall operation cost for the CO_2RR electrolysis.[44,48−50]

Compared with capturing and purifying CO_2 for the CO_2RR study above, directly employing diluted CO_2 streams as the feedstock could simplify these procedures and provide a more economical and energy-efficient route (Figure 1b). Nevertheless, how to achieve the unimpaired CO_2RR performance under such conditions still remains a formidable challenge. On the one hand, the low CO_2 concentration restricts the CO_2 mass transport and the formation of abundant three-phase interfaces, thereby causing a low efficiency for CO_2RR electrolysis and a rising selectivity for the competing hydrogen evolution reaction (HER).[51−54] On the other hand, there are some gas impurities such as reactive O_2 and SO_2 in industrial flue gas, which makes the direct electrochemical conversion of diluted CO_2 more complicated.[50,55,56] These gas impurities not only can compete with CO_2 for the reduction reactions but also probably affect the catalyst surface structures, which would result in the undesired reduction products and the deteriorated catalytic performance.[50,55,57] Therefore, it is very vital to develop some delicate design strategies for the achievement of efficient electroreduction of diluted CO_2 and gas impurities-tolerant CO_2RR.

3. DESIGN STRATEGIES FOR CO_2RR IN DILUTED CO_2

Direct utilization of diluted CO_2 can eliminate the need for the separate capture and enrichment of CO_2 from industrial flue gas, ultimately saving energy and simplifying the entire process. Nevertheless, this approach has significant obstacles because of the relatively low CO_2 concentration, which can decrease the CO_2 transport rate and increase the favored HER selectivity. To solve this challenge, interesting and diverse strategies have been employed to improve the local CO_2 concentration and increase the CO_2 partial pressure. In this section, we review and discuss some main strategies, including porous catalyst design, catalysts with functional groups, and coupling catalysts with other components.

3.1. Porous Catalysts. The preparation of porous catalysts with high specific surface areas is the simplest strategy to achieve the efficient CO_2RR in the low-concentration CO_2 condition.[52,58−61] Catalysts with porous structures can improve the physical adsorption of CO_2 molecules, thereby enriching the composition of CO_2 near the catalyst surfaces to promote the CO_2RR kinetics. For example, Jiang et al. reported the general synthesis of diverse single-atom metal sites on a porous N-doped carbon support (M−N−C) through a one-pot pyrolysis of metal−organic framework (MOF) precursors (Figure 2a).[59] The Ni−N−C catalyst exhibited the best CO_2R-to-CO activity with a CO Faradaic efficiency (FE) up to 96.8% in a pure CO_2 atmosphere, surpassing other Fe−N−C, Co−N−C, Cu−N−C, and N−C catalysts (Figure 2b). Using Ni−N−C as the catalyst, they further explored the CO_2RR performance in diluted CO_2 and found that this catalyst could reach a maximum CO FE of 91.6% in 30% CO_2, and even retain a CO FE of 83.2% at a lower CO_2 concentration of 15% (Figure 2c). This catalyst could operate stably over 10 h in diluted CO_2 condition. This good CO_2RR performance could be attributed to the microporous and mesoporous structures and abundant single-atom Ni active sites, which together promote the enrichment and electroreduction of diluted CO_2.

3.2. Catalysts with Functional Groups. Besides the above strategy of physical adsorption of CO_2, the introduction of specific CO_2-adsorption functional groups has been observed as an efficient approach to increase the CO_2 adsorption through a chemical bonding interaction.[5,62−65] For example, MOFs containing amine groups have been reported to have the capability in capturing CO_2 based on Lewis acid−base interactions.[66−69] Recently, Liao et al. reported the NH_2 group grafted on Ag-based MOF as a catalyst for the direct electroreduction of diluted CO_2 (Figure 2d).[69] To confirm the vital role of the NH_2 group, they synthesized three isostructural Ag-based MOFs with different functional groups of H, CH_3, and NH_2 (denoted as Ag-MOF, Ag-MOF-CH_3, and Ag-MOF-NH_2, respectively). The CO_2RR activity tests revealed that Ag-MOF-NH_2 achieved a CO partial current density of 355 mA cm^{-2} in 15% CO_2, slightly lower

https://doi.org/10.1021/acsnano.5c01268
ACS Nano 2025, 19, 10620−10629

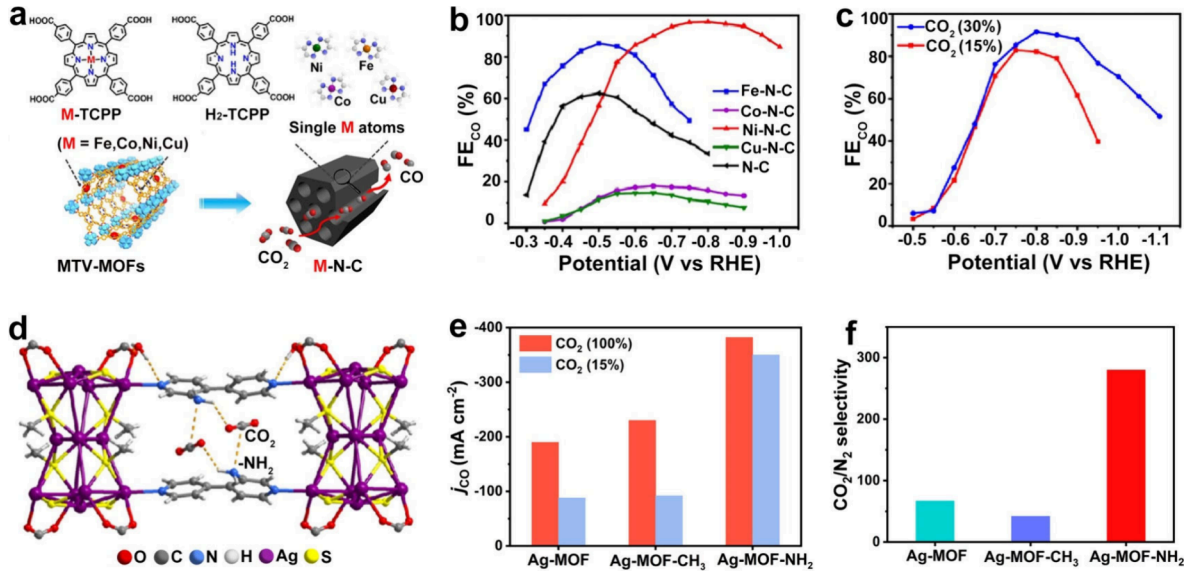

Figure 2. Some design strategies for the CO_2RR in diluted CO_2. (a) Schematic illustration of the general synthesis of porous M−N−C catalysts. (b) CO Faradaic efficiency of M−N−C catalysts in pure CO_2. (c) CO Faradaic efficiency of Ni−N−C catalyst in 30% and 15% CO_2. Reproduced with permission from ref 59. Copyright 2020, Wiley-VCH. (d) Schematic illustration of the interaction between the Ag-MOF-NH_2 catalyst and the CO_2 molecule. (e) Comparison of the CO partial current density for different catalysts in pure CO_2 and 15% CO_2. (f) CO_2/N_2 selectivity from CO_2/N_2 adsorption for different catalysts. Reproduced with permission from ref 69. Copyright 2023, Wiley-VCH.

than that of 380 mA cm^{-2} in pure CO_2, corresponding to 93.4% retention after the CO_2 partial pressure decreased by 85% (Figure 2e). In stark contrast, very low retention of a mere 44% and 37% was observed on Ag-MOF and Ag-MOF-CH_3 catalysts, respectively, suggesting that their CO_2RR activities were greatly affected by the altered CO_2 concentration. The CO_2/N_2 adsorption gave the CO_2/N_2 selectivity of 67, 42, and 280 at 298 K for Ag-MOF, Ag-MOF-CH_3, and Ag-MOF-NH_2, respectively (Figure 2f), indicative of the preferential adsorption of CO_2 on the NH_2 group. Therefore, the CO_2 was first captured by the NH_2 group through the N−C and H−O interactions (Figure 2d), and then the adsorbed CO_2 molecule migrated to the Ag cluster sites for the subsequent CO_2RR-to-CO conversion. In addition, other functional groups, such as imidazolium and quinone, have been also reported as the efficient CO_2 capture groups,[70−73] but their application for the CO_2RR in diluted CO_2 atmosphere is still lacking.

3.3. Coupling Catalysts with Other Components. As the grafting of functional groups would be limited by the specific catalysts, the incorporation of catalysts with some CO_2 adsorbents is a universal strategy to obtain the CO_2 enrichment.[38,54,74−76] On the basis of the binding interaction between amine molecule and CO_2, Kang et al. reported a composite catalyst by modifying tin oxide with diethanolamine (DEA) on carbon support (denoted as DEA-SnO_x/C, Figure 3a).[75] When the CO_2 concentration increased from 10% to 30%, the formate FE for DEA-SnO_x/C increased from 52% to 82%, and then the formate FE kept a stable value of ∼80% at a higher CO_2 concentration of >30% (Figure 3b). However, the SnO_x/C catalyst without the coupling of DEA exhibited the gradually increased formate FE when the CO_2 concentration increased from 10% to 100%. This prominent comparison shows that DEA-SnO_x/C could efficiently catalyze the CO_2R-to-formate at low CO_2 concentrations. The N 1s X-ray photoelectron spectroscopy revealed that the proportion of the peak at 399.9 eV increased from 43% to 63% after CO_2 adsorption (Figure 3c), arising from the combination of DEA and CO_2 to form the N−C=O bond. This observation was further verified by the in situ infrared spectroscopy characterization that the addition of DEA could help to stabilize the formation of the $CO_2{}^{*-}$ intermediate. A distinct peak from $CO_2{}^{*-}$ was observed on DEA-SnO_x/C, whereas there are no characteristic peaks from $CO_2{}^{*-}$ for SnO_x/C.

Apart from the amine molecule, ionic liquid (IL) has been reported as a promising media for CO_2 capture.[76−79] Although the addition of ILs into electrolyte could improve the CO_2 solubility in electrolyte, its low ionic conductivity and high viscosity can cause the poor mass transfer and high energy consumption.[77,79,80] Zhao et al. developed an interesting route to immobilize ILs into the pores of the Ni−N−C catalyst.[76] Seven ILs were successfully incorporated with the Ni−N−C catalyst (Figure 3d), and the Ni−N−C/[Bmim][PF_6] with high CO_2 adsorption exhibited optimal CO_2-to-CO activity with a maximum CO FE of 99.6% in pure CO_2. Compared with Ni−N−C, the Ni−N−C/[Bmim][PF_6] catalyst always exhibited larger current densities and higher CO FEs at different CO_2 concentrations (Figures 3e and 3f). Figure 3g further shows the defined increase factors of the CO partial current density after the introduction of [Bmim][PF_6]. A higher increase factor was observed at a lower CO_2 concentration, indicating the significant preconcentration of CO_2 in this ionic liquid. The mechanism study revealed that the hydrophobic chain of ILs can enrich CO_2 molecule and the in situ generated $CO_2{}^{*-}$ intermediate can coordinate with $[Bmim]^+$ cations to form [Bmim]-CO_2 complexes (Figure 3h). Therefore, the ILs here as the CO_2 concentrator and cocatalyst provide a low-energy pathway for the electroreduction of diluted CO_2 to produce CO. In addition, to reduce the catalyst flooding due to the solvation effect induced by ILs, Ye et al. proposed the covalent cross-link of ILs to form poly(ionic liquid), which was coated on the surface of Bi nanoparticles through in situ polymerization process.[81] The poly(ionic liquid) can increase the hydrophobicity of the catalyst, thus

https://doi.org/10.1021/acsnano.5c01268
ACS Nano 2025, 19, 10620−10629

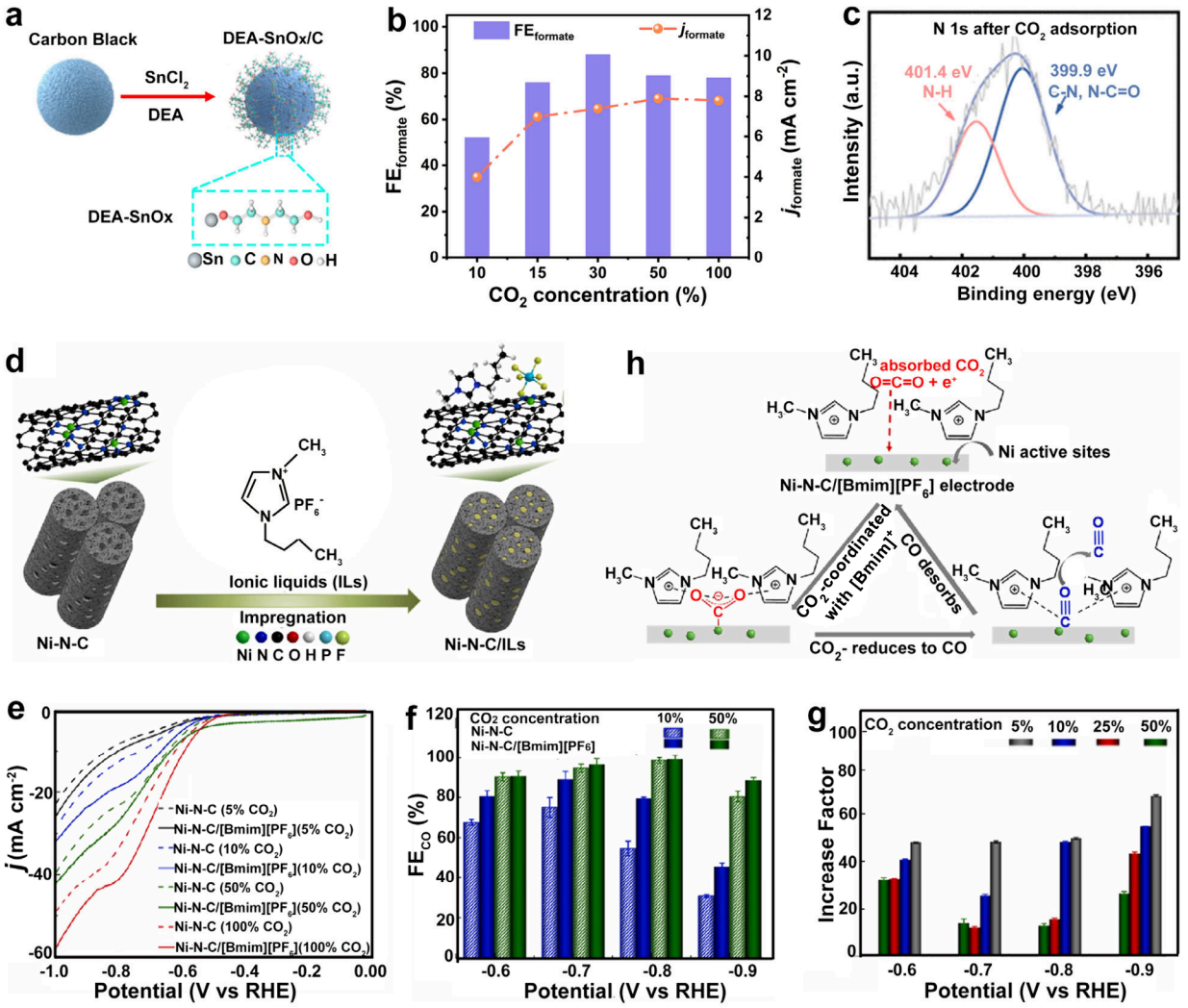

Figure 3. Coupling catalysts with other components for the CO_2RR in diluted CO_2. (a) Schematic illustration of the preparation process of DEA-SnO_x/C. (b) Formate Faradaic efficiency and partial current density for the DEA-SnO_x/C catalyst at different CO_2 concentrations. (c) N 1s X-ray photoelectron spectroscopy for the DEA-SnO_x/C catalyst after CO_2 adsorption. Reproduced with permission from ref 75. Copyright 2021, American Chemical Society. (d) Schematic illustration of the preparation process of Ni−N−C/IL composite catalysts. (e) CO_2RR polarization curves for Ni−N−C and Ni−N−C/[Bmim][PF_6] catalysts at different CO_2 concentrations. (f) CO Faradaic efficiency for Ni−N−C and Ni−N−C/[Bmim][PF_6] catalysts at different CO_2 concentrations. (g) The defined increase factors of CO partial current density after the introduction of [Bmim][PF_6] at different CO_2 concentrations. (h) Mechanism study for CO_2RR on Ni−N−C/[Bmim][PF_6] catalysts. Reproduced with permission from ref 76. Copyright 2022, Elsevier.

improving the CO_2 adsorption and local CO_2 concentration. The resulting catalyst could deliver a high formate FE of 90% over a wide potential range in simulated flue gas (15% CO_2).

4. DESIGN STRATEGIES FOR O_2/SO_2-TOLERANT CO_2RR

Although the direct utilization and electroreduction of diluted CO_2 could circumvent the CO_2 purification process, the actual component of industrial flue gas is relatively complex. Apart from the desired CO_2 gas, the flue gas also contains other gas impurities, such as O_2, SO_2, and so on.[55,82,83] Under the cathodic reduction conditions, these reactive gas molecules easily compete with CO_2, usually leading to the undesired reduction products and decreased CO_2RR selectivity.[50,55,57,84] Moreover, some gas impurities can alter the catalyst structures and surface properties, thereby causing the probably deteriorated activity and stability.[55] In this part, we will discuss the effect of O_2 and SO_2 impurities on the CO_2RR performance and catalyst structures and also summarize some interesting strategies for the O_2/SO_2-tolerant CO_2RR.

4.1. Design Strategies for O_2-Tolerant CO_2RR.

Generally, O_2 has the highest concentration of gas impurities in industrial flue gas and the O_2/CO_2 ratio is even greater than 20%.[34] Compared with CO_2RR, the oxygen reduction reaction (ORR) has a more positive reduction potential and requires a lower potential to drive it (e.g., $E^0(O_2/H_2O)$ = 1.23 V; $E^0(CO_2/CO)$ = − 0.11 V), thus resulting in the favored ORR over CO_2RR. For example, Sinton et al. studied the influence of O_2 impurities on the CO_2RR performance for Cu catalyst at high pressures (Figures 4a−4c).[50] They first found that increasing the pressure from 1 to 15 bar could efficiently improve the CO_2RR selectivity in 15% CO_2 without O_2 impurities. However, when fed with 4% O_2 in 15% CO_2 at 15 bar, prominently decreased FEs were observed over a wide voltage range for the bare Cu catalyst (Figure 4c), arising from the serious consumption of the applied current for ORR. It

https://doi.org/10.1021/acsnano.5c01268
ACS Nano 2025, 19, 10620−10629

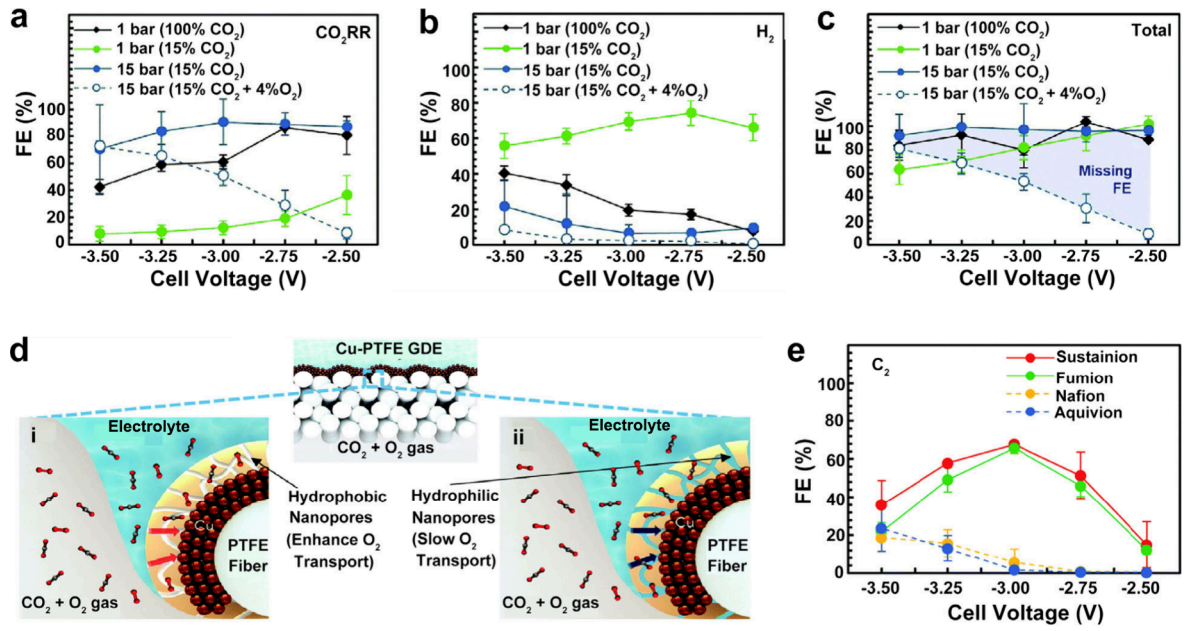

Figure 4. Design strategies for O_2-tolerant CO_2RR. (a) The CO_2RR Faradaic efficiency with the effect of O_2 impurities for the bare Cu catalyst. (b) The H_2 Faradaic efficiency with the effect of O_2 impurities for the bare Cu catalyst. (c) The total Faradaic efficiency with the effect of O_2 impurities for the bare Cu catalyst. (d) Schematic illustration of the hydrated ionomer coating strategy to lower the O_2 mass transport. (e) Faradaic efficiency toward multicarbon products for different ionomers-modified Cu in 15% CO_2 with 4% O_2. Reproduced with permission from ref 50. Copyright 2020, Royal Society of Chemistry.

could be attributed to the increased O_2 partial pressure and mass transport at higher pressures. They further designed a hydrated ionomer coating strategy to lower the rate of transport of the O_2 mass (Figure 4d). The hydrophobic nanopores can provide a fast gas diffusion pathway, whereas the hydrophilic nanopores promote the CO_2/O_2 gases dissolved in the electrolyte. Due to the volatile nature of O_2 in aqueous solutions, the O_2 mass flux is 10-fold slower in the hydrophilic nanopores than in the hydrophobic nanopores. In contrast, CO_2 has similar mass fluxes in the two nanopores, suggesting that the hydrophilic nanopores could selectively restrict O_2 transport but did not impact the CO_2 transport. Therefore, as shown in Figure 4e, two ionomer (Sustainion and Fumion) modified Cu catalysts with more hydrophilic nanopores exhibited higher CO_2RR FEs than those for two hydrophobic ionomers (Nafion and Aquivion). The highest FE of 68% for multicarbon products was achieved for the Sustainion ionomer at −3 V, indicating an efficient O_2-tolerant catalyst design for CO_2RR. Recently, Huang et al. reported a novel oxygen passivation strategy by employing a diarylethene (DEA) molecule, which could suppress the electron transfer between active sites and O_2 under the ring-closing form of DEA.[56] When fed with CO_2 and 5% O_2, the integration of cobalt porphyrin with DAE exhibited a high CO FE of 90.5%, much superior to that of 25.9% for the catalyst without DEA. The theoretical calculations revealed that the decorated DEA with close form has a poor O_2 activation capacity and a high *OOH formation energy, thereby resulting in a high energy barrier for the ORR.

4.2. Design Strategies for SO_2-Tolerant CO_2RR. SO_2 as another gas impurity has a typical concentration of ∼400 ppm in industrial flue gas.[85,86] Commonly, the reduction of SO_2 is thermodynamically more favorable than CO_2RR (e.g., $E^0(SO_2/S)$ = 0.5 V),[55] thus diminishing the CO_2RR selectivity. Moreover, the S poisoning phenomenon has been widely observed on many catalysts in diverse catalytic reactions.[57,87,88] Therefore, the effect of SO_2 impurities is more complicated compared with O_2 impurities. For example, Jiao et al. systematically investigated the effect of SO_2 impurities on CO_2RR performance and catalyst structures for Ag, Sn, and Cu catalysts (Figures 5a−5c).[55] When 1% SO_2 was mixed with CO_2, the total FEs toward the CO_2RR and HER decreased significantly for all catalysts (Figures 5d−5f), which is due to the charge consumption from SO_2 reduction. For Ag and Sn catalysts, SO_2 impurities can result in the in situ formation of a small amount of Ag_2S and SnS_2, respectively, but they did not change the product selectivity (Figures 5d and 5e). Meanwhile, their catalytic activities were fully recovered after removal of SO_2 impurities, indicative of a reversible process for these two catalysts. However, the case for Cu catalyst is totally different, and SO_2 impurities caused the obvious change of product selectivity from CO and multicarbon to formate (Figure 5f). When the SO_2 feed was stopped, formate remained the dominant CO_2RR product, suggesting that the Cu catalyst is highly sensitive to SO_2 impurities. Experimental characterizations and theoretical calculation results revealed that the in situ generation of Cu_2S on the Cu surface is likely responsible for the shifted product selectivity, and this Cu_2S species is very stable and could be detected even after 5 h of CO_2RR electrolysis.

Most recently, Papangelakis et al. constructed a polymer/catalyst/ionomer heterojunction to lower the *S coverage on Cu catalysts (Figure 5g).[44] In their design, the hydrophilic domains of perfluorosulfonic acid (PFSA) ionomer had a strong interaction with polar SO_2 and impeded its mass transport in the PFSA, while the hydrophobic chains of polytetrafluoroethylene (PTFE) could provide an unobstructed pathway for the fast transport of nonpolar CO_2. Therefore, via reaction−diffusion model analysis, the CO_2/SO_2 mass flux ratio for the modified Cu is nearly 2 orders of

https://doi.org/10.1021/acsnano.5c01268
ACS Nano 2025, 19, 10620−10629

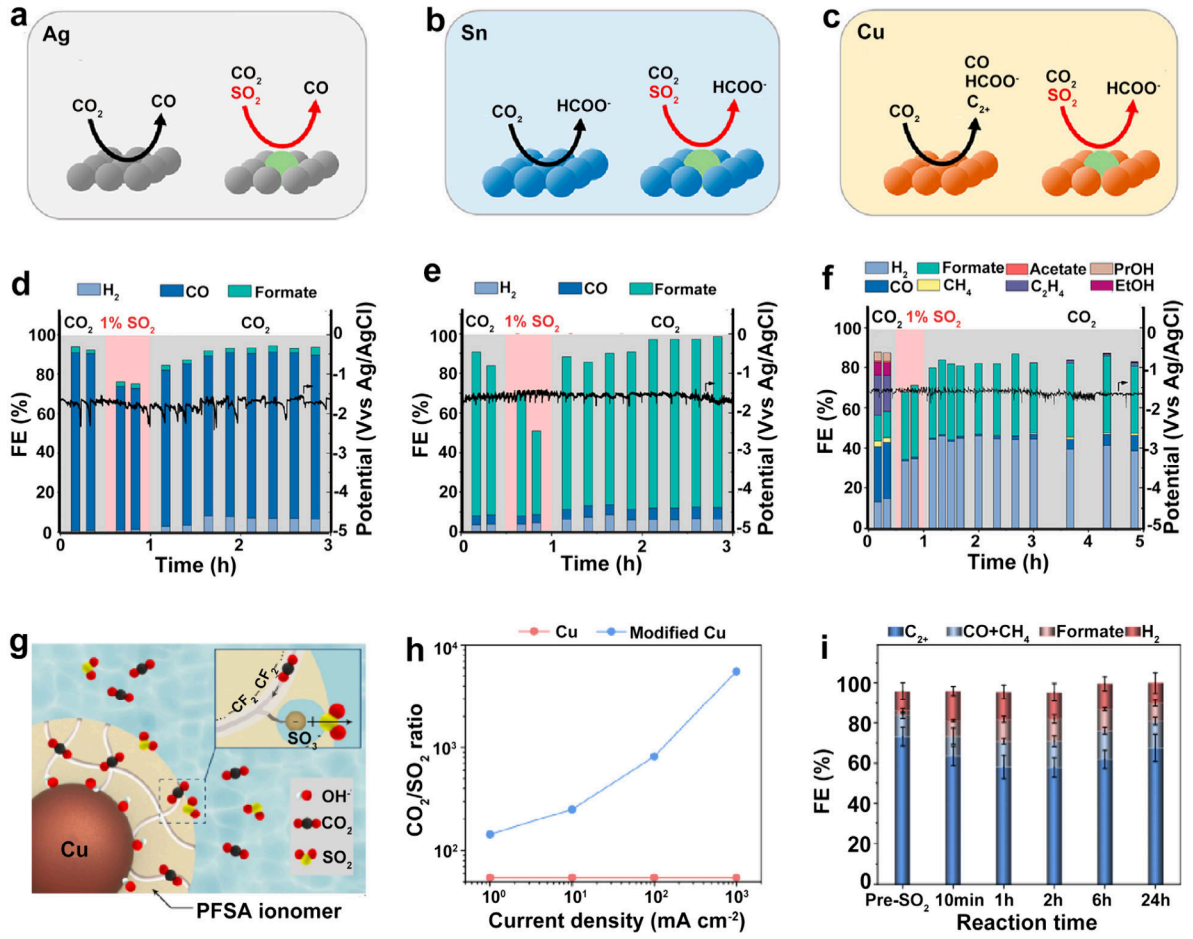

Figure 5. Design strategies for SO_2-tolerant CO_2RR. (a–c) Schematic illustration of the effect of SO_2 on the CO_2RR performance for (a) Ag, (b) Sn, and (c) Cu catalysts. (d–f) The CO_2RR Faradaic efficiency with the effect of 1% SO_2 for (d) Ag, (e) Sn, and (f) Cu catalysts. Reproduced with permission from ref 55. Copyright 2019, American Chemical Society. (g) Schematic illustration of a PFSA@Cu/PTFE heterojunction as the SO_2-tolerant CO_2RR catalyst. (h) Simulated CO_2/SO_2 mass flux ratio for bare Cu and modified Cu catalysts. (i) Product Faradaic efficiency for the designed PFSA@Cu/PTFE catalyst in 50% CO_2 with 400 ppm of SO_2. Reproduced with permission from ref 44. Copyright 2024, Springer Nature.

magnitude higher than that for the bare Cu (Figure 5h). This PFSA@Cu/PTFE catalyst exhibited a very excellent CO_2RR activity and durability in 50% CO_2 with 400 ppm of SO_2, delivering a high FE of over 60% for multicarbon products after 24 h of operation (Figure 5i). Furthermore, they demonstrated that this catalyst design strategy was valid in a simulated industrial flue gas condition containing 15% CO_2, 4% O_2, 500 ppm of NO, and 500 ppm of SO_2, which could achieve a prominent FE of ~50% for multicarbon products at 200 mA cm^{-2}.

5. CHALLENGES AND PERSPECTIVES

The direct electroreduction of diluted CO_2 (as in industrial flue gas) can eliminate the CO_2 capture and purification steps and avoid the additional energy consumption. Herein, we first briefly discuss the main advantages of the CO_2RR in diluted CO_2. We subsequently highlight some interesting design strategies and summarize their structure–performance relationship for the CO_2RR in diluted CO_2. Afterward, the effect of some gas impurities on the CO_2RR performance and several O_2/SO_2-tolerant catalyst designs are overviewed. Although much progress has been made in this field, more continued efforts are still required in the following several aspects.

5.1. New Design Strategies for Efficient CO_2RR in Diluted CO_2. The capture and enrichment of low-concentration CO_2 near the active sites of a catalyst is a crucial prerequisite to improve the local CO_2 concentrations, thus promoting the CO_2 conversion efficiencies. The CO_2 adsorption for previous reports mainly depends on the physical adsorption or chemical adsorption.[59,69,75,76,81] However, too weak physical adsorption (such as on porous carbon) easily results in CO_2-lacking environments, while too strong chemical adsorption (such as on amine-based media) might suppress the fast transport of CO_2 from adsorbents to active sites. The combination of physical and chemical adsorptions will be an alternative route to balance the CO_2 adsorption ability.[63,89] For example, Yaghi et al. recently reported an amine-group-decorated covalent organic framework (COF) as the CO_2 capture material.[63] Due to the high specific surface area of the COF and strong binding ability of amine-based groups, this material exhibits a high CO_2 uptake and good CO_2 adsorption–desorption cycles. We speculate that it will be very promising to use this kind of material as the support to further in situ grow active CO_2RR electrocatalysts for efficient reduction of diluted CO_2.

5.2. Understanding the Catalytic Mechanism in Diluted CO_2 Containing Gas Impurities. Although several

https://doi.org/10.1021/acsnano.5c01268
ACS Nano 2025, 19, 10620–10629

catalyst design strategies for O_2/SO_2-tolerant CO_2RR have been reported, the CO_2RR performance at these conditions is still worse than that without the gas impurities.[44,50,56,90] Nowadays, how these gas impurities affect the product selectivity and catalyst structure is still unclear. In addition, industrial flue gas also contains other gas impurities (such as NO and NO_2) and the concurrent existence of two or more gas impurities. But their impact on CO_2RR performance has rarely been investigated. We encourage more systematical studies to observe the catalyst structure changes and understand the actual deactivation mechanism at these conditions. For example, different operando characterization techniques, including electrochemical liquid-cell transmission electron microscopy (EC-TEM),[91,92] X-ray absorption spectroscopy,[92,93] Raman spectroscopy,[94,95] and infrared absorption spectroscopy,[96] have been employed to detect the catalyst dynamic evolution and reaction intermediates for electrocatalytic CO_2RR. For example, Zheng et al. used in situ EC-TEM to monitor the morphology and structural changes of Cu catalyst in real-time during the CO_2RR process. These operando techniques will help to explore more active catalysts and efficient approaches that permit operation of the CO_2RR under such harsh conditions.

5.3. CO_2RR in Acidic Media to Enhance Carbon Efficiency. The alkaline or neutral solutions are frequently used as the electrolytes for CO_2RR electrolysis, because the HER kinetics is 2−3 orders of magnitude slower in alkaline or neutral media than in acidic media.[97] However, the high-pH environment can cause serious carbon loss due to the carbonate formation.[28,98,99] The theoretical carbon efficiencies are <50% for the generation of CO or formate product and <25% for ethylene or ethanol product, meaning that more than 50% of input CO_2 is converted into carbonate but not for CO_2RR. Therefore, the local CO_2 concentration will be even lower when the diluted CO_2 is used. Operating the CO_2RR electrolysis in acidic media has been suggested to address the carbon loss problem, which can theoretically achieve the 100% carbon efficiency.[100−102] In recent years, researchers have developed a diverse range of strategies to suppress the competing HER in acid, such as catalyst structure and morphology tuning,[103−105] catalyst surface coating,[106,107] organic molecule and polymer modification,[108,109] and alkali cation enrichment.[28,98,110] Employing these useful strategies, the future direction is to conduct the electroreduction of diluted CO_2 in acidic electrolytes, which can totally settle the carbon loss issue to make full use of carbon sources for practical applications.

AUTHOR INFORMATION

Corresponding Authors

Zi-You Yu − *MOE International Joint Laboratory of Materials Microstructure, Institute for New Energy Materials and Low Carbon Technologies, School of Materials Science & Engineering, Tianjin University of Technology, Tianjin 300384, China;* orcid.org/0000-0002-8932-0814; Email: yuziyou@email.tjut.edu.cn

Tong-Bu Lu − *MOE International Joint Laboratory of Materials Microstructure, Institute for New Energy Materials and Low Carbon Technologies, School of Materials Science & Engineering, Tianjin University of Technology, Tianjin 300384, China;* orcid.org/0000-0002-6087-4880; Email: lutongbu@tjut.edu.cn

Authors

Jing-Jing Li − *MOE International Joint Laboratory of Materials Microstructure, Institute for New Energy Materials and Low Carbon Technologies, School of Materials Science & Engineering, Tianjin University of Technology, Tianjin 300384, China*

Xue-Rong Qin − *MOE International Joint Laboratory of Materials Microstructure, Institute for New Energy Materials and Low Carbon Technologies, School of Materials Science & Engineering, Tianjin University of Technology, Tianjin 300384, China*

Xiao-Ran Wang − *MOE International Joint Laboratory of Materials Microstructure, Institute for New Energy Materials and Low Carbon Technologies, School of Materials Science & Engineering, Tianjin University of Technology, Tianjin 300384, China*

Lin-Lin Wang − *MOE International Joint Laboratory of Materials Microstructure, Institute for New Energy Materials and Low Carbon Technologies, School of Materials Science & Engineering, Tianjin University of Technology, Tianjin 300384, China*

Complete contact information is available at: https://pubs.acs.org/10.1021/acsnano.5c01268

Author Contributions

[▽]J.-J.L. and X.-R.Q. contributed equally to this work.

Notes

The authors declare no competing financial interest.

ACKNOWLEDGMENTS

This work was supported by the National Key R&D Program of China (2022YFA1502902) and the National Natural Science Foundation of China (22375146 and 22109149).

REFERENCES

(1) Chang, B.; Pang, H.; Raziq, F.; Wang, S. B.; Huang, K. W.; Ye, J. H.; Zhang, H. B. Electrochemical reduction of carbon dioxide to multicarbon (C_{2+}) products: challenges and perspectives. *Energy Environ. Sci.* **2023**, *16*, 4714−4758.

(2) Allen, M. R.; Frame, D. J.; Huntingford, C.; Jones, C. D.; Lowe, J. A.; Meinshausen, M.; Meinshausen, N. Warming caused by cumulative carbon emissions towards the trillionth tonne. *Nature* **2009**, *458*, 1163−1166.

(3) Sanz-Pérez, E. S.; Murdock, C. R.; Didas, S. A.; Jones, C. W. Direct Capture of CO_2 from Ambient Air. *Chem. Rev.* **2016**, *116*, 11840−11876.

(4) Goeppert, A.; Czaun, M.; Surya Prakash, G. K.; Olah, G. A. Air as the renewable carbon source of the future: an overview of CO_2 capture from the atmosphere. *Energy Environ. Sci.* **2012**, *5*, 7833−7853.

(5) Shi, X.; Xiao, H.; Azarabadi, H.; Song, J.; Wu, X.; Chen, X.; Lackner, K. S. Sorbents for the Direct Capture of CO_2 from Ambient Air. *Angew. Chem., Int. Ed.* **2020**, *59*, 6984−7006.

(6) Li, X.; Wang, S.; Li, L.; Sun, Y.; Xie, Y. Progress and Perspective for In Situ Studies of CO_2 Reduction. *J. Am. Chem. Soc.* **2020**, *142*, 9567−9581.

(7) Lee, M. G.; Li, X. Y.; Ozden, A.; Wicks, J.; Ou, P. F.; Li, Y. H.; Dorakhan, R.; Lee, J. K. Y.; Park, H. K.; Yang, J. W.; Chen, B.; Abed, J.; dos Reis, R.; Lee, G. H.; Huang, J. E.; Peng, T.; Chin, Y. H.; Sinton, D.; Sargent, E. H. Selective synthesis of butane from carbon monoxide using cascade electrolysis and thermocatalysis at ambient conditions. *Nat. Catal.* **2023**, *6*, 310−318.

(8) Ramanathan, V.; Feng, Y. On avoiding dangerous anthropogenic interference with the climate system: Formidable challenges ahead. *Proc. Natl. Acad. Sci. U. S. A.* **2008**, *105*, 14245−14250.

(9) Navarro-Jaén, S.; Virginie, M.; Bonin, J.; Robert, M.; Wojcieszak, R.; Khodakov, A. Y. Highlights and challenges in the selective reduction of carbon dioxide to methanol. *Nat. Rev. Chem.* **2021**, *5*, 564−579.
(10) Cai, Y.; Lenton, T. M.; Lontzek, T. S. Risk of multiple interacting tipping points should encourage rapid CO_2 emission reduction. *Nat. Clim. Chang.* **2016**, *6*, 520−525.
(11) Jiang, Y.; Huang, L.; Chen, C.; Zheng, Y.; Qiao, S.-Z. Catalyst-electrolyte interface engineering propels progress in acidic CO_2 electroreduction. *Energy Environ. Sci.* **2025**, *18*, 2025−2049.
(12) Kibria, M. G.; Edwards, J. P.; Gabardo, C. M.; Dinh, C.-T.; Seifitokaldani, A.; Sinton, D.; Sargent, E. H. Electrochemical CO_2 Reduction into Chemical Feedstocks: From Mechanistic Electrocatalysis Models to System Design. *Adv. Mater.* **2019**, *31*, No. 1807166.
(13) Jiang, M.; Wang, H.; Zhu, M.; Luo, X.; He, Y.; Wang, M.; Wu, C.; Zhang, L.; Li, X.; Liao, X.; Jiang, Z.; Jin, Z. Review on strategies for improving the added value and expanding the scope of CO_2 electroreduction products. *Chem. Soc. Rev.* **2024**, *53*, 5149−5189.
(14) Gong, E.; Ali, S.; Hiragond, C. B.; Kim, H. S.; Powar, N. S.; Kim, D.; Kim, H.; In, S.-I. Solar fuels: research and development strategies to accelerate photocatalytic CO_2 conversion into hydrocarbon fuels. *Energy Environ. Sci.* **2022**, *15*, 880−937.
(15) Fang, S.; Rahaman, M.; Bharti, J.; Reisner, E.; Robert, M.; Ozin, G. A.; Hu, Y. H. Photocatalytic CO_2 reduction. *Nat. Rev. Method. Prim.* **2023**, *3*, 61.
(16) Mehla, S.; Kandjani, A. E.; Babarao, R.; Lee, A. F.; Periasamy, S.; Wilson, K.; Ramakrishna, S.; Bhargava, S. K. Porous crystalline frameworks for thermocatalytic CO_2 reduction: an emerging paradigm. *Energy Environ. Sci.* **2021**, *14*, 320−352.
(17) Hou, S.-L.; Dong, J.; Zhao, X.-Y.; Li, X.-S.; Ren, F.-Y.; Zhao, J.; Zhao, B. Thermocatalytic Conversion of CO_2 to Valuable Products Activated by Noble-Metal-Free Metal-Organic Frameworks. *Angew. Chem., Int. Ed.* **2023**, *62*, No. e202305213.
(18) Zhang, Y.-C.; Zhang, X.-L.; Wu, Z.-Z.; Niu, Z.-Z.; Chi, L.-P.; Gao, F.-Y.; Yang, P.-P.; Wang, Y.-H.; Yu, P.-C.; Duanmu, J.-W.; Sun, S.-P.; Gao, M.-R. Facet-switching of rate-determining step on copper in CO_2-to-ethylene electroreduction. *Proc. Natl. Acad. Sci. U. S. A.* **2024**, *121*, No. e2400546121.
(19) Rosen, B. A.; Salehi-Khojin, A.; Thorson, M. R.; Zhu, W.; Whipple, D. T.; Kenis, P. J. A.; Masel, R. I. Ionic Liquid-Mediated Selective Conversion of CO_2 to CO at Low Overpotentials. *Science* **2011**, *334*, 643−645.
(20) Jin, S.; Hao, Z.; Zhang, K.; Yan, Z.; Chen, J. Advances and Challenges for the Electrochemical Reduction of CO_2 to CO: From Fundamentals to Industrialization. *Angew. Chem., Int. Ed.* **2021**, *60*, 20627−20648.
(21) Ross, M. B.; De Luna, P.; Li, Y.; Dinh, C.-T.; Kim, D.; Yang, P.; Sargent, E. H. Designing materials for electrochemical carbon dioxide recycling. *Nat. Catal.* **2019**, *2*, 648−658.
(22) Nitopi, S.; Bertheussen, E.; Scott, S. B.; Liu, X. Y.; Engstfeld, A. K.; Horch, S.; Seger, B.; Stephens, I. E. L.; Chan, K.; Hahn, C.; Norskov, J. K.; Jaramillo, T. F.; Chorkendorff, I. Progress and Perspectives of Electrochemical CO_2 Reduction on Copper in Aqueous Electrolyte. *Chem. Rev.* **2019**, *119*, 7610−7672.
(23) Yang, P.-P.; Gao, M.-R. Enrichment of reactants and intermediates for electrocatalytic CO_2 reduction. *Chem. Soc. Rev.* **2023**, *52*, 4343−4380.
(24) Lei, Y.; Wang, Z.; Bao, A.; Tang, X.; Huang, X.; Yi, H.; Zhao, S.; Sun, T.; Wang, J.; Gao, F. Recent advances on electrocatalytic CO_2 reduction to resources: Target products, reaction pathways and typical catalysts. *Chem. Eng. J.* **2023**, *453*, No. 139663.
(25) Wei, P.; Gao, D.; Liu, T.; Li, H.; Sang, J.; Wang, C.; Cai, R.; Wang, G.; Bao, X. Coverage-driven selectivity switch from ethylene to acetate in high-rate CO_2/CO electrolysis. *Nat. Nanotechnol.* **2023**, *18*, 299−306.
(26) Gu, J.; Hsu, C. S.; Bai, L. C.; Chen, H. M.; Hu, X. L. Atomically dispersed Fe^{3+} sites catalyze efficient CO_2 electroreduction to CO. *Science* **2019**, *364*, 1091−1094.
(27) Fang, W.; Guo, W.; Lu, R.; Yan, Y.; Liu, X.; Wu, D.; Li, F. M.; Zhou, Y.; He, C.; Xia, C.; Niu, H.; Wang, S.; Liu, Y.; Mao, Y.; Zhang, C.; You, B.; Pang, Y.; Duan, L.; Yang, X.; Song, F.; Zhai, T.; Wang, G.; Guo, X.; Tan, B.; Yao, T.; Wang, Z.; Xia, B. Y. Durable CO_2 conversion in the proton-exchange membrane system. *Nature* **2024**, *626*, 86−91.
(28) Huang, J. E.; Li, F.; Ozden, A.; Sedighian Rasouli, A.; Garcia de Arquer, F. P.; Liu, S.; Zhang, S.; Luo, M.; Wang, X.; Lum, Y.; Xu, Y.; Bertens, K.; Miao, R. K.; Dinh, C.-T.; Sinton, D.; Sargent, E. H. CO_2 electrolysis to multicarbon products in strong acid. *Science* **2021**, *372*, 1074−1078.
(29) Jiang, Z. N.; Ren, S.; Cao, X.; Fan, Q. K.; Yu, R.; Yang, J.; Mao, J. J. pH-Universal Electrocatalytic CO_2 Reduction with Ampere-Level Current Density on Doping-Engineered Bismuth Sulfide. *Angew. Chem., Int. Ed.* **2024**, *63*, No. e202408412.
(30) García de Arquer, F. P.; Dinh, C.-T.; Ozden, A.; Wicks, J.; McCallum, C.; Kirmani, A. R.; Nam, D.-H.; Gabardo, C.; Seifitokaldani, A.; Wang, X.; Li, Y. C.; Li, F.; Edwards, J.; Richter, L. J.; Thorpe, S. J.; Sinton, D.; Sargent, E. H. CO_2 electrolysis to multicarbon products at activities greater than 1 A cm^{-2}. *Science* **2020**, *367*, 661−666.
(31) Wang, H.; Liu, Y.; Laaksonen, A.; Krook-Riekkola, A.; Yang, Z.; Lu, X.; Ji, X. Carbon recycling-An immense resource and key to a smart climate engineering: A survey of technologies, cost and impurity impact. *Renew. Sust. Energy Rev.* **2020**, *131*, No. 110010.
(32) Boot-Handford, M. E.; Abanades, J. C.; Anthony, E. J.; Blunt, M. J.; Brandani, S.; Mac Dowell, N.; Fernández, J. R.; Ferrari, M.-C.; Gross, R.; Hallett, J. P.; Haszeldine, R. S.; Heptonstall, P.; Lyngfelt, A.; Makuch, Z.; Mangano, E.; Porter, R. T. J.; Pourkashanian, M.; Rochelle, G. T.; Shah, N.; Yao, J. G.; Fennell, P. S. Carbon capture and storage update. *Energy Environ. Sci.* **2014**, *7*, 130−189.
(33) Jin, S. J.; Wu, M.; Gordon, R. G.; Aziz, M. J.; Kwabi, D. G. pH swing cycle for CO_2 capture electrochemically driven through proton-coupled electron transfer. *Energy Environ. Sci.* **2020**, *13*, 3706−3722.
(34) D'Alessandro, D. M.; Smit, B.; Long, J. R. Carbon Dioxide Capture: Prospects for New Materials. *Angew. Chem., Int. Ed.* **2010**, *49*, 6058−6082.
(35) Shin, H.; Hansen, K. U.; Jiao, F. Techno-economic assessment of low-temperature carbon dioxide electrolysis. *Nat. Sustain.* **2021**, *4*, 911−919.
(36) Sullivan, I.; Goryachev, A.; Digdaya, I. A.; Li, X.; Atwater, H. A.; Vermaas, D. A.; Xiang, C. Coupling electrochemical CO_2 conversion with CO_2 capture. *Nat. Catal.* **2021**, *4*, 952−958.
(37) Sharifian, R.; Wagterveld, R. M.; Digdaya, I. A.; Xiang, C.; Vermaas, D. A. Electrochemical carbon dioxide capture to close the carbon cycle. *Energy Environ. Sci.* **2021**, *14*, 781−814.
(38) Chu, S. Carbon Capture and Sequestration. *Science* **2009**, *325*, 1599−1599.
(39) Keith, D. W.; Holmes, G.; St. Angelo, D.; Heidel, K. A Process for Capturing CO_2 from the Atmosphere. *Joule* **2018**, *2*, 1573−1594.
(40) Wei, W.; Li, D.; Yan, X.; Mu, X.; Li, Z.; Liu, Z. Novel DETA-Isobutanol biphasic solvent for post-combustion CO_2 capture: High cyclic capacity and low energy consumption. *Carbon Capture Sci. Technol.* **2024**, *13*, No. 100235.
(41) Popielak, P.; Majchrzak-Kucęba, I.; Wawrzyńczak, D. Climate change mitigation with CCUS-A case study with benchmarking for selected countries in adapting the European Union's Green Deal. *Int. J. Greenh. Gas Con.* **2024**, *132*, No. 104057.
(42) Wang, M.; Luo, J. A coupled electrochemical system for CO_2 capture, conversion and product purification. *eScience* **2023**, *3*, No. 100155.
(43) Buckingham, J.; Reina, T. R.; Duyar, M. S. Recent advances in carbon dioxide capture for process intensification. *Carbon Capture Sci. Technol.* **2022**, *2*, No. 100031.
(44) Papangelakis, P.; Miao, R. K.; Lu, R.; Liu, H.; Wang, X.; Ozden, A.; Liu, S.; Sun, N.; O'Brien, C. P.; Hu, Y.; Shakouri, M.; Xiao, Q.; Li, M.; Khatir, B.; Huang, J. E.; Wang, Y.; Xiao, Y. C.; Li, F.; Zeraati, A. S.; Zhang, Q.; Liu, P.; Golovin, K.; Howe, J. Y.; Liang, H.; Wang, Z.; Li, J.; Sargent, E. H.; Sinton, D. Improving the SO_2 tolerance of CO_2

https://doi.org/10.1021/acsnano.5c01268
ACS Nano 2025, 19, 10620−10629

reduction electrocatalysts using a polymer/catalyst/ionomer heterojunction design. *Nat. Energy* **2024**, *9*, 1011−1020.
(45) Zhang, X.; Fang, Z.; Zhu, P.; Xia, Y.; Wang, H. Electrochemical regeneration of high-purity CO_2 from (bi)carbonates in a porous solid electrolyte reactor for efficient carbon capture. *Nat. Energy* **2025**, *10*, 55−65.
(46) Keith, D. W.; Holmes, G.; St. Angelo, D.; Heidel, K. A Process for Capturing CO_2 from the Atmosphere. *Joule* **2018**, *2*, 1573−1594.
(47) Liu, M.; Zhan, L.; Wang, Y.; Zhao, X.; Wu, J.; Deng, D.; Jiang, J.; Zheng, X.; Lei, Y. Achieving integrated capture and reduction of CO_2: A promising electrocatalyst. *J. Mater. Sci. Technol.* **2023**, *165*, 235−243.
(48) Service, R. F. Cost of carbon capture drops, but does anyone want it? *Science* **2016**, *354*, 1362−1363.
(49) Ho, M. T.; Allinson, G. W.; Wiley, D. E. Factors affecting the cost of capture for Australian lignite coal fired power plants. *Energy Procedia* **2009**, *1*, 763−770.
(50) Xu, Y.; Edwards, J. P.; Zhong, J.; O'Brien, C. P.; Gabardo, C. M.; McCallum, C.; Li, J.; Dinh, C.-T.; Sargent, E. H.; Sinton, D. Oxygen-tolerant electroproduction of C_2 products from simulated flue gas. *Energy Environ. Sci.* **2020**, *13*, 554−561.
(51) Wang, X.; Xu, A.; Li, F.; Hung, S.-F.; Nam, D.-H.; Gabardo, C. M.; Wang, Z.; Xu, Y.; Ozden, A.; Rasouli, A. S.; Ip, A. H.; Sinton, D.; Sargent, E. H. Efficient methane electrosynthesis enabled by tuning local CO_2 availability. *J. Am. Chem. Soc.* **2020**, *142*, 3525−3531.
(52) Hou, P.; Song, W.; Wang, X.; Hu, Z.; Kang, P. Well-Defined Single-Atom Cobalt Catalyst for Electrocatalytic Flue Gas CO_2 Reduction. *Small* **2020**, *16*, No. 2001896.
(53) Dinh, C.-T.; Burdyny, T.; Kibria, M. G.; Seifitokaldani, A.; Gabardo, C. M.; García de Arquer, F. P.; Kiani, A.; Edwards, J. P.; De Luna, P.; Bushuyev, O. S.; Zou, C.; Quintero-Bermudez, R.; Pang, Y.; Sinton, D.; Sargent, E. H. CO_2 electroreduction to ethylene via hydroxide-mediated copper catalysis at an abrupt interface. *Science* **2018**, *360*, 783−787.
(54) Chen, B.; Rong, Y.; Li, X.; Sang, J.; Wei, P.; An, Q.; Gao, D.; Wang, G. Molecular Enhancement of Direct Electrolysis of Dilute CO_2. *ACS Energy Lett.* **2024**, *9*, 911−918.
(55) Luc, W.; Ko, B. H.; Kattel, S.; Li, S.; Su, D.; Chen, J. G. G.; Jiao, F. SO_2-Induced Selectivity Change in CO_2 Electroreduction. *J. Am. Chem. Soc.* **2019**, *141*, 9902−9909.
(56) Zhu, H.-J.; Si, D.-H.; Guo, H.; Chen, Z.; Cao, R.; Huang, Y.-B. Oxygen-tolerant CO_2 electroreduction over covalent organic frameworks via photoswitching control oxygen passivation strategy. *Nat. Commun.* **2024**, *15*, 1479.
(57) Lim, J. W.; Dong, W. J.; Cho, W. S.; Yoo, C. J.; Lee, J.-L. CuS_x Catalysts by Ag-Mediated Corrosion of Cu for Electrochemical Reduction of Sulfur-Containing CO_2 Gas to HCOOH. *ACS Catal.* **2022**, *12*, 13174−13185.
(58) Nie, B.; Xiong, X.-W.; Xu, X.-D.; Cheng, Y.-S.; Yu, D.; Kang, Y.-S.; Wu, K.-L.; Wu, F.-H.; Yuan, G.; Wei, X.-W. Tailoring the hierarchical porous nitrogen-doped carbon structures loaded single-atomic Ni catalyst for promoting CO_2 electrochemical reduction at low CO_2 concentration. *Inorg. Chem. Commun.* **2023**, *153*, No. 110876.
(59) Jiao, L.; Yang, W.; Wan, G.; Zhang, R.; Zheng, X.; Zhou, H.; Yu, S.-H.; Jiang, H.-L. Single-Atom Electrocatalysts from Multivariate Metal-Organic Frameworks for Highly Selective Reduction of CO_2 at Low Pressures. *Angew. Chem., Int. Ed.* **2020**, *59*, 20589−20595.
(60) Ding, M.; Liu, X.; Ma, P.; Yao, J. Porous materials for capture and catalytic conversion of CO_2 at low concentration. *Coord. Chem. Rev.* **2022**, *465*, No. 214576.
(61) Zhang, Y.; Ding, L.; Xie, Z.; Zhang, X.; Sui, X.; Li, J.-R. Porous sorbents for direct capture of carbon dioxide from ambient air. *Chin. Chem. Lett.* **2025**, *36*, No. 109676.
(62) Lyu, H.; Li, H.; Hanikel, N.; Wang, K.; Yaghi, O. M. Covalent Organic Frameworks for Carbon Dioxide Capture from Air. *J. Am. Chem. Soc.* **2022**, *144*, 12989−12995.
(63) Zhou, Z. H.; Ma, T. Q.; Zhang, H. Y.; Chheda, S.; Li, H. Z.; Wang, K. Y.; Ehrling, S.; Giovine, R.; Li, C. S.; Alawadhi, A. H.; Abduljawad, M. M.; Alawad, M. O.; Gagliardi, L.; Sauer, J.; Yaghi, O. M. Carbon dioxide capture from open air using covalent organic frameworks. *Nature* **2024**, *635*, 96−101.
(64) Zhao, Z.-H.; Huang, J.-R.; Huang, D.-S.; Zhu, H.-L.; Liao, P.-Q.; Chen, X.-M. Efficient Capture and Electroreduction of Dilute CO_2 into Highly Pure and Concentrated Formic Acid Aqueous Solution. *J. Am. Chem. Soc.* **2024**, *146*, 14349−14356.
(65) Wang, D.; Mao, J.; Zhang, C.; Zhang, J.; Li, J.; Zhang, Y.; Zhu, Y. Modulating microenvironments to enhance CO_2 electroreduction performance. *eScience* **2023**, *3*, No. 100119.
(66) Chen, S.; Han, X.; Sun, X.; Luo, X.; Liang, Z. The comparative kinetics study of CO_2 absorption into non-aqueous DEEA/MEA and DMEA/MEA blended systems solution by using stopped-flow technique. *Chem. Eng. J.* **2020**, *386*, No. 121295.
(67) Zhang, R.; He, X.; Liu, T.; Li, C. e.; Xiao, M.; Ling, H.; Hu, X.; Zhang, X.; Tang, F.; Luo, H. a. Thermodynamic studies for improving the prediction of CO_2 equilibrium solubility in aqueous 2-dimethylamino-2-methyl-1-propanol. *Sep. Purif. Technol.* **2022**, *295*, No. 121292.
(68) Ding, M.; Flaig, R. W.; Jiang, H.-L.; Yaghi, O. M. Carbon capture and conversion using metal-organic frameworks and MOF-based materials. *Chem. Soc. Rev.* **2019**, *48*, 2783−2828.
(69) Liu, Y. Y.; Huang, J. R.; Zhu, H. L.; Liao, P. Q.; Chen, X. M. Simultaneous Capture of CO_2 Boosting Its Electroreduction in the Micropores of a Metal-organic Framework. *Angew. Chem., Int. Ed.* **2023**, *62*, No. e202311265.
(70) Xue, L.; Gao, Z.; Ning, T.; Li, W.; Li, J.; Yin, J.; Xiao, L.; Wang, G.; Zhuang, L. Dual-Role of Polyelectrolyte-Tethered Benzimidazolium Cation in Promoting CO_2/Pure Water Co-Electrolysis to Ethylene. *Angew. Chem., Int. Ed.* **2023**, *62*, No. e202309519.
(71) Kim, C.; Bui, J. C.; Luo, X.; Cooper, J. K.; Kusoglu, A.; Weber, A. Z.; Bell, A. T. Tailored catalyst microenvironments for CO_2 electroreduction to multicarbon products on copper using bilayer ionomer coatings. *Nat. Energy* **2021**, *6*, 1026−1034.
(72) Abdinejad, M.; Massen-Hane, M.; Seo, H.; Hatton, T. A. Oxygen-Stable Electrochemical CO_2 Capture using Redox-Active Heterocyclic Benzodithiophene Quinone. *Angew. Chem., Int. Ed.* **2024**, *63*, No. e202412229.
(73) Yang, L.; Shi, C.; Li, L.; Li, Y. High-throughput model-building and screening of zeolitic imidazolate frameworks for CO_2 capture from flue gas. *Chin. Chem. Lett.* **2020**, *31*, 227−230.
(74) Kim, S.-M.; Kim, K.-M.; Choi, B.-K.; Mun, J.-H.; Shin, B.-J.; Lee, U.; Shin, C.-H.; Choi, J.; Min, B.-M.; Lee, U.; Moon, J.-H. CO2 absorption mechanism in aqueous ternary solutions of alkanolamines: Experimental and thermodynamic modeling approaches. *Chem. Eng. J.* **2022**, *428*, No. 132044.
(75) Cheng, Y.; Hou, J.; Kang, P. Integrated Capture and Electroreduction of Flue Gas CO_2 to Formate Using Amine Functionalized SnO_x Nanoparticles. *ACS Energy Lett.* **2021**, *6*, 3352−3358.
(76) Sun, Q.; Zhao, Y.; Ren, W.; Zhao, C. Electroreduction of low concentration CO_2 at atomically dispersed Ni-N-C catalysts with nanoconfined ionic liquids. *Appl. Catal. B: Environ.* **2022**, *304*, No. 120963.
(77) Zhang, S.; Zhang, J.; Zhang, Y.; Deng, Y. Nanoconfined Ionic Liquids. *Chem. Rev.* **2017**, *117*, 6755−6833.
(78) Dongare, S.; Zeeshan, M.; Aydogdu, A. S.; Dikki, R.; Kurtoğlu-Öztulum, S. F.; Coskun, O. K.; Muñoz, M.; Banerjee, A.; Gautam, M.; Ross, R. D.; Stanley, J. S.; Brower, R. S.; Muchharla, B.; Sacci, R. L.; Velázquez, J. M.; Kumar, B.; Yang, J. Y.; Hahn, C.; Keskin, S.; Morales-Guio, C. G.; Uzun, A.; Spurgeon, J. M.; Gurkan, B. Reactive capture and electrochemical conversion of CO_2 with ionic liquids and deep eutectic solvents. *Chem. Soc. Rev.* **2024**, *53*, 8563−8631.
(79) Avila, J.; Lepre, L. F.; Santini, C. C.; Tiano, M.; Denis-Quanquin, S.; Chung Szeto, K.; Padua, A. A. H.; Costa Gomes, M. High-Performance Porous Ionic Liquids for Low-Pressure CO_2 Capture. *Angew. Chem., Int. Ed.* **2021**, *60*, 12876−12882.
(80) Asadi, M.; Kim, K.; Liu, C.; Addepalli, A. V.; Abbasi, P.; Yasaei, P.; Phillips, P.; Behranginia, A.; Cerrato, J. M.; Haasch, R.; Zapol, P.;

https://doi.org/10.1021/acsnano.5c01268
ACS Nano 2025, 19, 10620−10629

Kumar, B.; Klie, R. F.; Abiade, J.; Curtiss, L. A.; Salehi-Khojin, A. Nanostructured transition metal dichalcogenide electrocatalysts for CO_2 reduction in ionic liquid. *Science* **2016**, *353*, 467−470.
(81) Li, G.; Zhang, C.; Liu, Y.; Song, Y.; Guo, W.; Huang, L.; Su, J.; Zhang, Q.; Xin, Y.; Feng, T.; Cao, X.; He, M.; Kwok, T. K.; Lam, J. W. Y.; Jin, Z.; Tang, B. Z.; Wang, Z.; Ye, R. Molecular Engineering of Poly(Ionic Liquid) for Direct and Continuous Production of Pure Formic Acid from Flue Gas. *Adv. Mater.* **2024**, *36*, No. 2409390.
(82) Zhang, H.; Wang, Z.; Wei, L.; Liu, Y.; Dai, H.; Deng, J. Recent progress on VOC pollution control via the catalytic method. *Chin. J. Catal.* **2024**, *61*, 71−96.
(83) Tian, D.; Qu, Z.; Zhang, J. Electrochemical condition optimization and techno-economic analysis on the direct CO_2 electroreduction of flue gas. *Appl. Energy* **2023**, *351*, No. 121787.
(84) Wang, N. N.; Jiang, W. B.; Yang, J.; Feng, H. S.; Zheng, Y. B.; Wang, S.; Li, B. F.; Heng, J. Z. X.; Ong, W. C.; Tan, H. R.; Zhang, Y. W.; Wang, D. A.; Ye, E. Y.; Li, Z. B. Contact-electro-catalytic CO_2 reduction from ambient air. *Nat. Commun.* **2024**, *15*, 5913.
(85) Lee, J. Y.; Keener, T. C.; Yang, Y. J. Potential Flue Gas Impurities in Carbon Dioxide Streams Separated from Coal-Fired Power Plants. *J. Air Waste Manage. Assoc.* **2009**, *59*, 725−732.
(86) Gao, J. B.; Wang, S. J.; Zhao, B.; Qi, G. J.; Chen, C. H. Pilot-Scale Experimental Study on the CO_2 Capture Process with Existing of SO_2: Degradation, Reaction Rate, and Mass Transfer. *Energy Fuels* **2011**, *25*, 5802−5809.
(87) Feng, S.; Jiang, M.; Song, X.; Qiao, P.; Yan, L.; Cai, Y.; Li, B.; Li, C.; Ning, l.; Liu, S.; Zhang, W.; Wu, G.; Yang, J.; Dong, W.; Yang, X.; Jiang, Z.; Ding, Y. Sulfur Poisoning and Self-Recovery of Single-Site Rh_1/Porous Organic Polymer Catalysts for Olefin Hydroformylation. *Angew. Chem., Int. Ed.* **2023**, *62*, No. e202304282.
(88) Han, X.; Liu, K.; Bian, M.; Yuan, Z.; Li, Y.; Zhang, Y.; Yang, X.; Zhang, Y. SO_2-induced surface defects on monatomic Ce-doped $MoTiO_x$ catalyst for efficient reduction of NO_x with NH_3. *Appl. Catal. B: Environ.* **2025**, *366*, No. 125021.
(89) Hsu, K.-J.; Li, S.; Micari, M.; Chi, H.-Y.; Villalobos, L. F.; Huang, S.; Zhong, L.; Song, S.; Duan, X.; Züttel, A.; Agrawal, K. V. Graphene membranes with pyridinic nitrogen at pore edges for high-performance CO_2 capture. *Nat. Energy* **2024**, *9*, 964−974.
(90) Xiao, Y. C.; Sun, S. S.; Zhao, Y.; Miao, R. K.; Fan, M.; Lee, G.; Chen, Y.; Gabardo, C. M.; Yu, Y.; Qiu, C.; Guo, Z.; Wang, X.; Papangelakis, P.; Huang, J. E.; Li, F.; O'Brien, C. P.; Kim, J.; Han, K.; Corbett, P. J.; Howe, J. Y.; Sargent, E. H.; Sinton, D. Reactive capture of CO_2 via amino acid. *Nat. Commun.* **2024**, *15*, 7849.
(91) Zhang, Q.; Song, Z.; Sun, X.; Liu, Y.; Wan, J.; Betzler, S. B.; Zheng, Q.; Shangguan, J.; Bustillo, K. C.; Ercius, P.; Narang, P.; Huang, Y.; Zheng, H. Atomic dynamics of electrified solid−liquid interfaces in liquid-cell TEM. *Nature* **2024**, *630*, 643−647.
(92) Yang, Y.; Louisia, S.; Yu, S.; Jin, J.; Roh, I.; Chen, C.; Fonseca Guzman, M. V.; Feijóo, J.; Chen, P.-C.; Wang, H.; Pollock, C. J.; Huang, X.; Shao, Y.-T.; Wang, C.; Muller, D. A.; Abruña, H. D.; Yang, P. Operando studies reveal active Cu nanograins for CO_2 electroreduction. *Nature* **2023**, *614*, 262−269.
(93) DuanMu, J.-W.; Wu, Z.-Z.; Gao, F.-Y.; Yang, P.-P.; Niu, Z.-Z.; Zhang, Y.-C.; Chi, L.-P.; Gao, M.-R. Investigation and Mitigation of Carbon Deposition over Copper Catalyst during Electrochemical CO_2 Reduction. *Precis. Chem.* **2024**, *2*, 151−160.
(94) Handoko, A. D.; Wei, F. X.; Jenndy; Yeo, B. S.; Seh, Z. W. Understanding heterogeneous electrocatalytic carbon dioxide reduction through operando techniques. *Nat. Catal.* **2018**, *1*, 922−934.
(95) Niu, Z.-Z.; Chi, L.-P.; Wu, Z.-Z.; Yang, P.-P.; Fan, M.-H.; Gao, M.-R. CO_2-assisted formation of grain boundaries for efficient CO-CO coupling on a derived Cu catalyst. *Natl. Sci. Open* **2023**, *2*, No. 20220044.
(96) Zhang, Z. M.; Wang, T.; Cai, Y. C.; Li, X. Y.; Ye, J. Y.; Zhou, Y.; Tian, N.; Zhou, Z. Y.; Sun, S. G. Probing electrolyte effects on cation-enhanced CO_2 reduction on copper in acidic media. *Nat. Catal.* **2024**, *7*, 807−817.
(97) Subbaraman, R.; Tripkovic, D.; Strmcnik, D.; Chang, K.-C.; Uchimura, M.; Paulikas, A. P.; Stamenkovic, V.; Markovic, N. M. Enhancing Hydrogen Evolution Activity in Water Splitting by Tailoring Li^+-$Ni(OH)_2$-Pt Interfaces. *Science* **2011**, *334*, 1256−1260.
(98) Gu, J.; Liu, S.; Ni, W.; Ren, W.; Haussener, S.; Hu, X. Modulating electric field distribution by alkali cations for CO_2 electroreduction in strongly acidic medium. *Nat. Catal.* **2022**, *5*, 268−276.
(99) Li, Y.-C.; Zhang, X.-L.; Tai, X.-L.; Yang, X.-P.; Yu, P.-C.; Dong, S.-C.; Chi, L.-P.; Wu, Z.-Z.; Zhang, Y.-C.; Sun, S.-P.; Lu, P.-G.; Zhu, L.; Gao, F.-Y.; Lin, Y.; Gao, M.-R. Highly Tension-Strained Copper Concentrates Diluted Cations for Selective Proton-Exchange Membrane CO_2 Electrolysis. *Angew. Chem., Int. Ed.* **2025**, *64*, No. e202422054.
(100) Wu, W. X.; Xu, L. P.; Lu, Q.; Sun, J. P.; Xu, Z. Y.; Song, C. S.; Yu, J. C.; Wang, Y. Addressing the Carbonate Issue: Electrocatalysts for Acidic CO_2 Reduction Reaction. *Adv. Mater.* **2025**, *37*, No. 2312894.
(101) Zeng, M.; Fang, W.; Cen, Y.; Zhang, X.; Hu, Y.; Xia, B. Y. Reaction Environment Regulation for Electrocatalytic CO_2 Reduction in Acids. *Angew. Chem., Int. Ed.* **2024**, *63*, No. e202404574.
(102) Jiang, Y.; Li, H.; Chen, C.; Zheng, Y.; Qiao, S.-Z. Dynamic Cu^0/Cu^+ Interface Promotes Acidic CO_2 Electroreduction. *ACS Catal.* **2024**, *14*, 8310−8316.
(103) Xie, Y.; Ou, P.; Wang, X.; Xu, Z.; Li, Y. C.; Wang, Z.; Huang, J. E.; Wicks, J.; McCallum, C.; Wang, N.; Wang, Y.; Chen, T.; Lo, B. T. W.; Sinton, D.; Yu, J. C.; Wang, Y.; Sargent, E. H. High carbon utilization in CO_2 reduction to multi-carbon products in acidic media. *Nat. Catal.* **2022**, *5*, 564−570.
(104) Sun, M.; Cheng, J.; Yamauchi, M. Gas diffusion enhanced electrode with ultrathin superhydrophobic macropore structure for acidic CO_2 electroreduction. *Nat. Commun.* **2024**, *15*, 491.
(105) Chi, L.-P.; Niu, Z.-Z.; Zhang, Y.-C.; Zhang, X.-L.; Liao, J.; Wu, Z.-Z.; Yu, P.-C.; Fan, M.-H.; Tang, K.-B.; Gao, M.-R. Efficient and stable acidic CO_2 electrolysis to formic acid by a reservoir structure design. *Proc. Natl. Acad. Sci. U. S. A.* **2023**, *120*, No. e2312876120.
(106) Li, L.; Liu, Z.; Yu, X.; Zhong, M. Achieving High Single-Pass Carbon Conversion Efficiencies in Durable CO_2 Electroreduction in Strong Acids via Electrode Structure Engineering. *Angew. Chem., Int. Ed.* **2023**, *62*, No. e202300226.
(107) Zhao, Y.; Hao, L.; Ozden, A.; Liu, S.; Miao, R. K.; Ou, P.; Alkayyali, T.; Zhang, S.; Ning, J.; Liang, Y.; Xu, Y.; Fan, M.; Chen, Y.; Huang, J. E.; Xie, K.; Zhang, J.; O'Brien, C. P.; Li, F.; Sargent, E. H.; Sinton, D. Conversion of CO_2 to multicarbon products in strong acid by controlling the catalyst microenvironment. *Nat. Synth.* **2023**, *2*, 403−412.
(108) Nie, W.; Heim, G. P.; Watkins, N. B.; Agapie, T.; Peters, J. C. Organic Additive-derived Films on Cu Electrodes Promote Electrochemical CO_2 Reduction to C_{2+} Products Under Strongly Acidic Conditions. *Angew. Chem., Int. Ed.* **2023**, *62*, No. e202216102.
(109) Fan, M.; Huang, J. E.; Miao, R. K.; Mao, Y.; Ou, P.; Li, F.; Li, X.-Y.; Cao, Y.; Zhang, Z.; Zhang, J.; Yan, Y.; Ozden, A.; Ni, W.; Wang, Y.; Zhao, Y.; Chen, Z.; Khatir, B.; O'Brien, C. P.; Xu, Y.; Xiao, Y. C.; Waterhouse, G. I. N.; Golovin, K.; Wang, Z.; Sargent, E. H.; Sinton, D. Cationic-group-functionalized electrocatalysts enable stable acidic CO_2 electrolysis. *Nat. Catal.* **2023**, *6*, 763−772.
(110) Zi, X.; Zhou, Y.; Zhu, L.; Chen, Q.; Tan, Y.; Wang, X.; Sayed, M.; Pensa, E.; Geioushy, R. A.; Liu, K.; Fu, J.; Cortés, E.; Liu, M. Breaking K^+ Concentration Limit on Cu Nanoneedles for Acidic Electrocatalytic CO_2 Reduction to Multi-Carbon Products. *Angew. Chem., Int. Ed.* **2023**, *62*, No. e202309351.

https://doi.org/10.1021/acsnano.5c01268
ACS Nano 2025, 19, 10620−10629